Biosensors and Bioelectronics 41 (2013) 232–237

Contents lists available at SciVerse ScienceDirect

Biosensors and Bioelectronics

journal homepage: www.elsevier.com/locate/bios

The utility of a high-throughput scanning biosensor in the detection of the pancreatic cancer marker ULBP2

Ying-Feng Chang [a,b,1], Jau-Song Yu [a,c,1], Ya-Ting Chang [a], Li-Chen Su [b], Chih-Ching Wu [a,e], Yu-Sun Chang [a,c], Chao-Sung Lai [d,f], Chien Chou [b,f,*]

[a] Molecular Medicine Research Center, Chang Gung University, Taoyuan 33302, Taiwan
[b] Graduate Institute of Electro-Optical Engineering, Chang Gung University, Taoyuan 33302, Taiwan
[c] Graduate Institute of Biomedical Science, Chang Gung University, Taoyuan 33302, Taiwan
[d] Department of Electronic Engineering, Chang Gung University, Taoyuan 33302, Taiwan
[e] Department of Medical Biotechnology and Laboratory Science, Chang Gung University, Taoyuan 33302, Taiwan
[f] Center for Biomedical Engineering, Chang Gung University, Taoyuan 33302, Taiwan

ARTICLE INFO

Article history:
Received 4 June 2012
Received in revised form
7 August 2012
Accepted 10 August 2012
Available online 23 August 2012

Keywords:
ULBP2
High-throughput detection
Localized surface plasmon
Metal-enhanced fluorescence

ABSTRACT

In this study, a novel high-throughput biosensor based on metal-enhanced fluorescence technique and harmonic intensity-modulated fluorescence technique was developed and demonstrated to be highly sensitive for the detection of a pancreatic cancer marker, UL16-binding protein 2 (ULBP2), in diluted serum. Experimentally, the biosensor is able to detect ULBP2 at 16–18 pg/mL in 1% BSA–PBS and in 10-fold-diluted human serum. Compared with the limit of detection (LOD) of the conventional enzyme-linked immunosorbent assay (ELISA) method, the LOD of the proposed biosensor for ULBP2 is significantly improved by 100-fold under the same conditions. In addition, the proposed method uses two identical polyclonal antibodies for the sandwich immunoassay, simplifying the experiment in terms of the reagents needed. Consequently, this biosensor is a cost-effective tool for clinical diagnosis. We believe that the proposed high-throughput biosensor has great potential to become a clinical diagnostic tool for the detection of a pancreatic cancer marker in the near future.

1. Introduction

Pancreatic cancer (PC) is a highly lethal malignancy with a nearly 100% mortality; an estimated 43,920 new cases and 37,390 deaths in the United States were reported by the National Cancer Institute"-body in 2012. Despite advances in powerful imaging techniques such as computed tomography (CT), magnetic resonance imaging (MRI), endoscopic retrograde cholangiopancreatography (ERCP), and endoscopic ultrasound (EUS), most tumors are not detected sufficiently early to benefit from surgery (Chakraborty et al., 2011; Bezabeh et al., 2009). Only 5–25% of patients presenting with pancreatic cancer have operable tumors, highlighting the importance of early detection utilizing biomarkers (Pliarchopoulou and Pectasides 2009; Li et al., 2009). Cancer antigen 19-9 (CA 19-9), a carbohydrate antigen present in serum, is widely used as a tumor marker for PC. However, it has not been used for diagnostic purposes because of its low specificity and sensitivity (Bezabeh et al., 2009; Chang et al., 2011b). This limitation has led investigators to search for and identify other biomarkers, such as plectin-1, macrophage inhibitory cytokine-1, IGFBP-1, haptoglobin, SAA, TIMP-1, HE4, NGAL, and particularly human UL16-binding protein 2 (ULBP2), for PC screening (Chang et al., 2011b; Bausch et al., 2011; Brand et al., 2011; Goggins, 2011).

In our previous study (Chang et al., 2011b), we reported that the serum level of ULBP2 is significantly elevated in PC patients compared with that in healthy controls. Most importantly, the combined use of ULBP2 and CA 19-9 improved the sensitivity and accuracy of early PC detection and thus provided promising results for early PC diagnosis. Unfortunately, the ULBP2 concentration in the serum of healthy controls is approximately 50 pg/mL, which is difficult to precisely measure with the commercial enzyme-linked immunosorbent assay (ELISA) (Chang et al., 2011(b)). To our knowledge, only a few groups have been able to measure ULBP2 in human serum by utilizing either exceptional antibodies or a bead-based immunoassay with a flow cytometer (Chang et al., 2011b; Paschen et al., 2009; Waldhauer and Steinle, 2006; Linkov et al., 2009). Therefore, we sought to develop a novel and cost-effective high-throughput biosensor with high sensitivity for ULBP2 detection in diluted human serum because the detection of this marker is crucial for the early diagnosis of PC.

In recent years, gold nanoparticles (GNPs) have been introduced to enhance the detection sensitivity of biosensors and have become

* Corresponding author at: Graduate Institute of Electro-Optical Engineering, Chang Gung University, Taoyuan 33302, Taiwan. Tel.: +886 3 2118 800x3677; fax: +886 3 2118 507.
E-mail address: cchou@mail.cgu.edu.tw (C. Chou).
[1] Equal contributions to this research.

0956-5663/$ - see front matter © 2012 Elsevier B.V. All rights reserved.
http://dx.doi.org/10.1016/j.bios.2012.08.026

one of the most efficient tools for clinical diagnosis (Ho et al., 2010; Soo et al., 2009). GNPs possess special optical characteristics such as localized surface plasmons (LSPs), which is the collective oscillation of the electron cloud induced by interaction with an electromagnetic field. The LSPs of GNPs exhibit wavelength-selective absorption with an extremely large molar extinction coefficient, which results in a high density of electric fields near the surface of GNPs within 50–60 nm (Anker et al., 2008; Willets and Van Duyne, 2007; Sagle et al., 2011; Jones et al., 2011; Rycenga et al., 2011; Hartland, 2011). In our previously developed localized surface plasmon coupled fluorescence fiber-optic biosensor (LSPCF-FOB), GNP was used in combination with a sandwich immunoassay to study protein–protein interactions (Hsieh et al., 2007; Ng and Liu, 2009; Huang et al., 2009; Chang et al., 2009; 2010 ; 2011a; Su et al., 2011). The features of the LSPCF-FOB that provide high sensitivity and specificity include (1) the metal-enhanced fluorescence, (2) amplification of the fluorescence signal by a number of fluorophores on a single LSPCF probe, and (3) the sandwich immunoassay configuration. However, the LSPCF-FOB is not compatible with high-throughput capability, which is required for clinical diagnostic purposes.

In this study, a novel high-throughput localized surface plasmon coupled harmonic fluorescence biosensor (HT-LSPCHFB) was proposed and developed. This biosensor integrates the features of (a) high-throughput detection, (b) sandwich immunoassay-based measurements, (c) metal-enhanced fluorescence, and (d) the optical heterodyne technique. The HT-LSPCHFB has the distinguishing characteristic that the fluorescence is excited and harmonic intensity-modulated via heterodyne interference. Besides, a ratio algorithm was adopted in this setup for the simultaneously detected fluorescence and reference heterodyne signals. This significantly reduces the excess noise from laser intensity fluctuation and improves the sensitivity of HT-LSPCHFB. Additionally, the LSP is excited directly by the laser beam in free space in the HT-LSPCHFB rather than by an evanescent wave generated in an optical fiber in the LSPCF-FOB. The use of the laser beam in free space greatly simplifies the optical setup and allows the detection of multiple ligands.

In this experiment, the detection on a novel PC marker, ULBP2, in 1% BSA–PBS and in 10-fold-diluted human serum was demonstrated. The HT-LSPCHFB not only has a high detection sensitivity and specificity but also requires fewer expensive reagents because it uses two identical polyclonal antibodies in a sandwich immunoassay. Therefore, this biosensor is based on a cost-effective high-throughput sandwich immunoassay.

2. Materials and methods

2.1. Materials

Human serum was prepared from a healthy donor. The polyclonal antibody (goat anti-human ULBP2), which is used as the capture antibody and the detection antibody, was purchased from R&D Systems (Minneapolis, MN, USA). The purified human ULBP2 protein, used as the target antigen, was also purchased from R&D Systems. In addition, bovine serum albumin (BSA) and phosphate-buffered saline (PBS) were purchased from Sigma (St. Louis, MO, USA). Additionally, GNP-conjugated streptavidin (Au–SA, GNP diameter ~25 nm) was obtained from Aurion (Wageningen, Netherlands), and the fluorescence labeling kit (Lightning-Link® Atto633) and the biotin labeling kit were obtained from Innova Biosciences (Cambridge, UK). Alkaline phosphatase-conjugated streptavidin and 4-methylumbelliferyl phosphate were purchased from Amersham Biosciences (Uppsala, Sweden) and Molecular Probes, Inc. (Eugene, OR, USA), respectively. Finally, the 96-well immunoplates were obtained from Corning Costar (Corning, NY, USA).

2.2. Preparation of the LSPCF probes

Biotin- and fluorophore-labeled detection antibodies bound to Au–SA was used as a LSPCF probe, as shown in Fig. 1A. The detection antibody was conjugated to biotin and the fluorophore using commercial labeling kits from Innova Biosciences. The fluorophore (Lightning-Link® Atto633) showed strong absorption at 629 nm and a maximum fluorescence emission at 657 nm. To produce the LSPCF probes, 2.06 μg/mL of the detection antibody was mixed with Au–SA at a concentration of 8.49×10^9 particles/mL and then incubated for more than 10 h at 4 °C in the dark.

2.3. Optical setup and use of the HT-LSPCHFB

The optical setup of the HT-LSPCHFB is shown in Fig. 1B. A two-frequency laser with a 632.8 nm wavelength was used as an excitation light source. This laser outputs a pair of orthogonal linear polarization with a slight difference in the temporal frequency (2 kHz), which can be generated using a frequency-stabilized linear polarized He–Ne laser associated with an electro-optical modulator (New Focus 4002) that is driven by a 2 kHz sawtooth signal (Su et al., 1996; Yu et al., 2008; 2009). In this

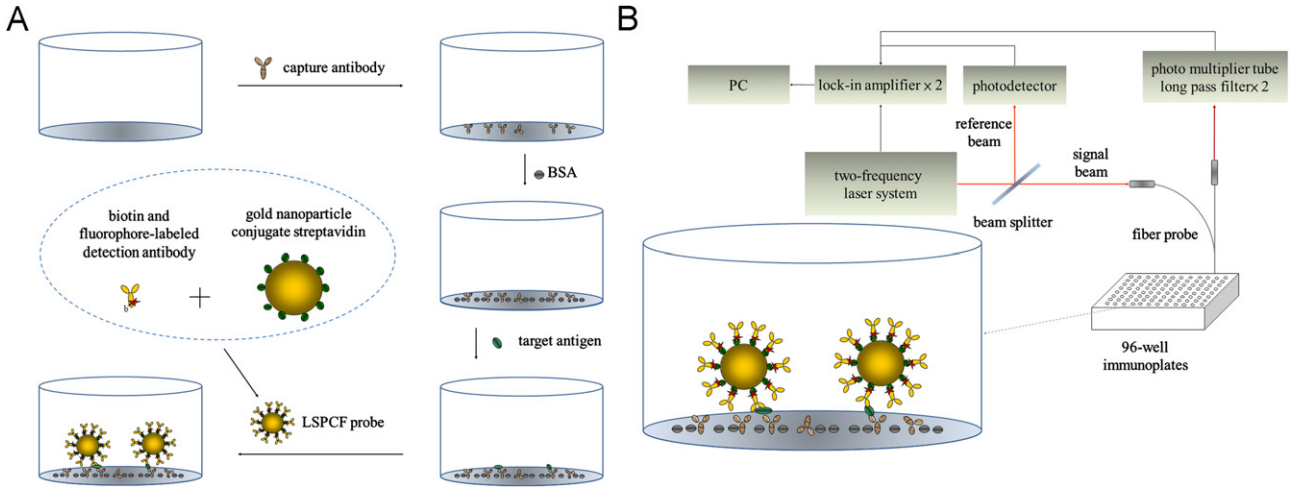

Fig. 1. (A) The sandwich immunocomplexes and the LSPCF probes and (B) optical setup of the HT-LSPCHFB.

measurement, we chose 2 K as modulation frequency due to the appropriate modulation index of the heterodyne signal generated whereas, the optimized frequency is determined by the highest modulation index of the heterodyne signal obtained in this setup. In addition to that, $1/f$ noise which is inversely proportional to the modulation frequency is also reduced. There is a beam splitter to split the two-frequency laser beam into a signal beam and a reference beam. The signal beam is incident to a single well of the 96-well immunoplate in which the $<$capture antibody/target antigen/LSPCF probe$>$ immunocomplex is constructed, as shown in Fig. 1A. LSPCF probes are then excited by the two-frequency laser beam, and a harmonic intensity-modulated fluorescence signal is generated via heterodyne interference. Two identical long-pass filters (cutoff wavelength = 640 nm) are introduced to this setup to detect the harmonic-modulated fluorescence signal via a photomultiplier tube. Simultaneously, the demodulated intensities of the harmonic-modulated fluorescence signal and the heterodyned reference signal are measured separately using two lock-in amplifiers. The ratio of the demodulated fluorescence signal and the reference signal is monitored during measurement to reduce excess noise of the system.

2.4. Stability of the HT-LSPCHFB

At first, the background and reference signals were monitored by continuously measuring a single well of a 96-well immunoplate filled with 100 μL of PBS for 3 h. The background signal was obtained by measuring the back scattering signal via a photomultiplier tube (PMT), and the reference signal was detected by measuring the laser intensity of the reference beam with a photodetector. In the meantime, the variation among the wells of the 96-well immunoplate was tested and analyzed.

2.5. Human ULBP2 measurement in PBS solution using conventional ELISA

We utilized two identical polyclonal antibodies (goat anti-human ULBP2) as the capture antibody and the detection antibody for the conventional ELISA. First, the capture antibody was immobilized on the bottom surface of each well by adding 50 μL at a 6 μg/mL concentration (~300 ng/well) at room temperature for 2 h. The immunoplate was then washed six times with PBS. Then, each well was filled with 100 μL of 1% BSA in PBS (1% BSA–PBS) to block unoccupied sites on the surface of each well for 2 h at room temperature. After washing, serial dilutions of ULBP2 in 1% BSA–PBS in a 50 μL volume were independently added to the 96 wells, and then the plate was incubated at room temperature for another 2 h. The immunoplate was then washed six times with PBS. The biotinylated detection antibody (50 μL), diluted 1:500 in 1% BSA–PBS, was added to each well, followed by 2 h incubation at room temperature. After six washes, 50 μL of streptavidinylated alkaline phosphatase diluted 1:3000 in PBS was added to each well, and the plates were incubated at room temperature for 2 h. The immunoplate was then washed six times with PBS. Finally, 100 μM 4-methylumbelliferyl phosphate (100 μL/well) was added to each well as a substrate, and the fluorescence intensity (excitation: 355 nm, emission: 460 nm) was measured using a SpectraMax M5 microplate reader (Molecular Devices; Sunnyvale, CA, USA).

2.6. Measurement of human ULBP2 in PBS or in diluted human serum using the HT-LSPCHFB

The experimental preparation for detection of ULBP2 utilizing the HT-LSPCHFB was similar to that of the previously mentioned ELISA method. Briefly, 96-well immunoplates were first coated with 100 μL of 3 μg/mL (~300 ng/well) capture antibody at 4 °C overnight. They were then washed six times with PBS. After the immunoplates were blocked with 100 μL of 1% BSA–PBS for 1 h at 37 °C, serial dilutions of ULBP2 in 1% BSA–PBS or in a 10-fold-diluted human serum in a total volume of 100 μL were separately added in the wells, and the plates were incubated at room temperature for 2 h. The immunoplates were then washed six times with PBS again. Finally, 100 μL of the LSPCF probe solution was added to each well, followed by a 2 h incubation at room temperature to form the $<$capture antibody/ULBP2/LSPCF probe$>$ immunocomplex on the bottom surface of each well, as shown in Fig. 1A. After washing six times with PBS, the immunoplates were measured by the HT-LSPCHFB. This assay is conducted in parallel using a conventional 96-well immunoplate, requiring a scanning time of 15 min for all 96 samples.

2.7. Data analysis

All fitting curves were analyzed with the GraphPad Prism software to fit a non-linear regression using a four-parameter dose-response curve (variable slope model), which is defined by,

$$Y = B + \frac{A-B}{1+10^{((\log C - X)D)}} \quad (1)$$

where Y is the signal, X is the analyte concentration, A is the highest signal, B is the lowest signal, C is the concentration corresponding to the half-maximal signal, and D describes the steepness of the calibration curve. Generally, the limit of detection (LOD) is the concentration at which the signal corresponding to three times the sd (standard deviation of the blank measurement without the target antigen) is positioned in the dose–response curve.

3. Results and discussion

3.1. Stability of the HT-LSPCHFB system

The temporal stability was analyzed using the background and reference signals, which were monitored by continuously measuring a single well of the 96-well immunoplate filled with 100 μL PBS solution for 3 h (Fig. 2A). The downside drift of both the background (blue points) and reference (red points) signals might be caused by system noise such as laser intensity fluctuations during the measurement. The drift and noise produced by laser intensity fluctuations can be significantly reduced by using the ratio of the background signal and the reference beam during the measurement, thereby improving the temporal stability of the HT-LSPCHFB system. The system background signal (SBS, green points) measured when using the ratio algorithm is shown in Fig. 2(A). The ration algorithm results in much better stability than the use of the background signal without the ratio algorithm. The stability of the HT-LSPCHFB system was also calculated as the percentage error based on continuous SBS monitoring for 3 h, where the percentage error is defined as,

$$\text{percentageerror} = \frac{\text{SBS} - M_{\text{SBS}}}{M_{\text{SBS}}} \quad (2)$$

where M_{SBS} is the mean value of SBS. Fig. 2(B) presents the percent error of the SBS for the HT-LSPCHFB spanning 3 h. The fluctuation was less than $\pm 2\%$ in this experiment.

3.2. Measurement of human ULBP2 in PBS using conventional ELISA

We first set up a conventional sandwich ELISA using two identical polyclonal antibodies (goat anti-human ULBP2 for both

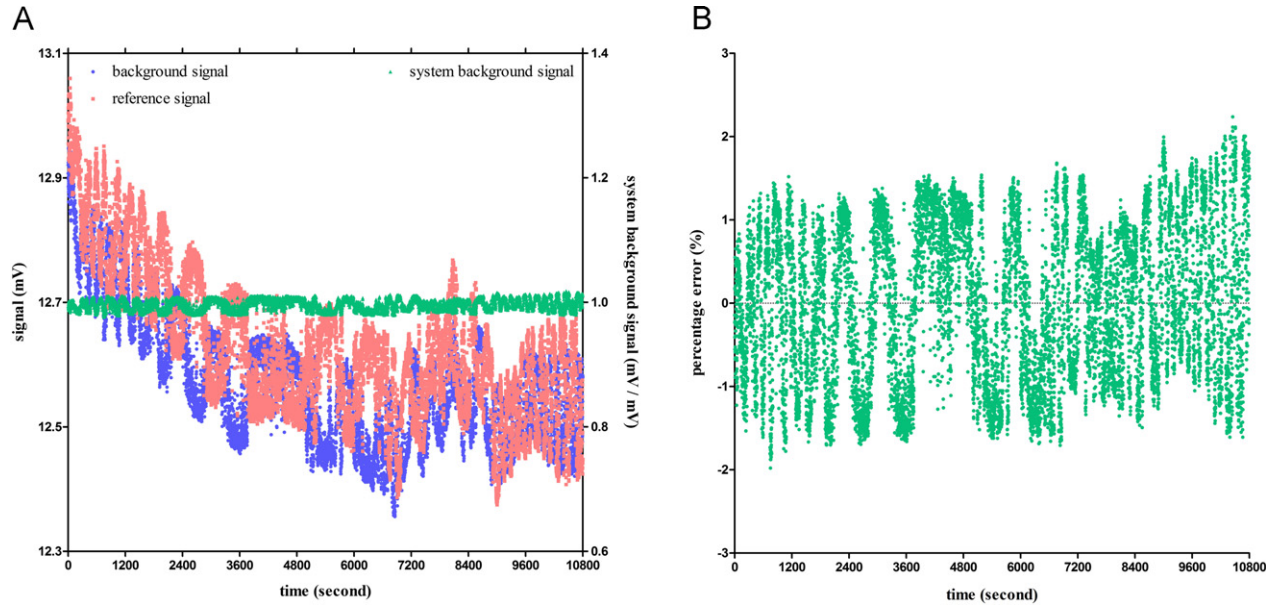

Fig. 2. (A) The background (blue), reference signal (red) and system background signal (green) were monitored by continuously measuring one well of a 96-well immunoplate filled with 100 μL of PBS for 3 h. System background signal (green) is the ratio of the background signal (blue) and the reference signal (red) during the measurement. (B) The temporal stability of the HT-LSPCHFB was calculated and monitored as the percent error using the system background signal. (For interpretation of the references to color in this figure legend, the reader is referred to the web version of this article.)

the capture antibody and the detection antibody) against human ULBP2, the antigen, to evaluate the sensitivity of the sandwich immunoassay. Fig. 3 shows the four-parameter dose–response relationship between the signal and the concentrations of ULBP2 in 1% BSA–PBS, where the concentration ranged from 0 ng/mL to 250 ng/mL. In this experiment, the correlation coefficient (R^2) was 0.9977, and the detection sensitivity is estimated to be 2 ng/mL. According to a previous study, the serum ULBP2 concentrations in PC patients and healthy controls were 200 pg/mL and 50 pg/mL, respectively (Chang et al., 2011b). These results indicate that the conventional sandwich ELISA is not suitable for early PC diagnosis.

3.3. *Measurement of human ULBP2 in PBS and diluted human serum using the HT-LSPCHFB*

To develop a highly sensitive assay for ULBP2 detection, we used the HT-LSPCHFB to measure ULBP2 both in 1% BSA–PBS and in diluted human serum independently. Different dilutions of ULBP2 in 1% BSA–PBS (0 pg/mL, 0.1 pg/mL, 1 pg/mL, 10 pg/mL, 100 pg/mL, 1 ng/mL, and 10 ng/mL) were added to a 96-well immunoplate to form a < capture antibody/target antigen/LSPCF probe > immunocomplex. The harmonic intensity-modulated fluorescence signal from each well was measured. The result is shown in Fig. 4, which presents the four-parameter dose-response relationship between the normalized fluorescence signal and the ULBP2 concentration over the range of 0.1 pg/mL–10 ng/mL. The correlation coefficient (R^2) was 0.9738. The error bar indicates one standard deviation for five repetitions. The "normalized fluorescence signal" on the y-axis in Fig. 4 is equal to the measured fluorescence intensity minus the background level for each measurement. The fluorescence signal was normalized based on the demodulated amplitude of the heterodyne signal in the reference channel. This treatment of the data reduces the level of excess noise from the laser intensity fluctuations during measurement. The LOD was estimated to be 18.0 pg/mL for the HT-LSPCHFB in this experiment.

To demonstrate that the HT-LSPCHFB can be applied to clinical specimens, we spiked ULBP2 into 10-fold-diluted serum. Fig. 5

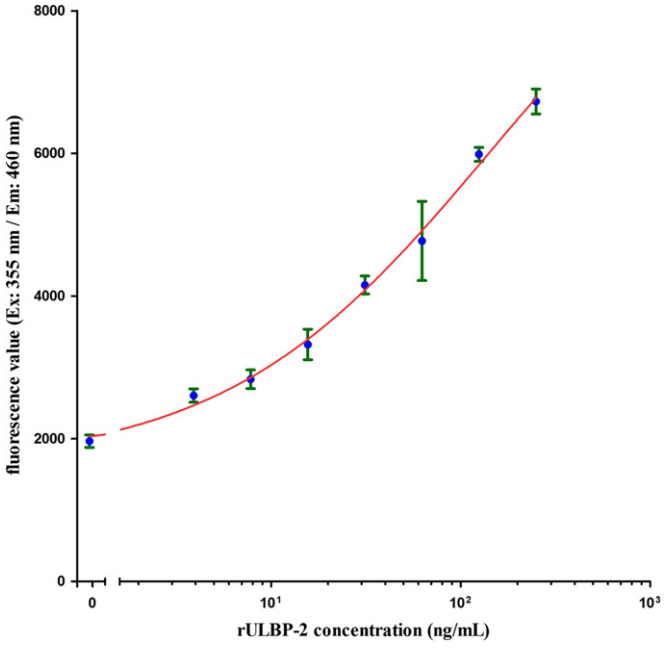

Fig. 3. The four-parameter dose–response relationship (R^2=0.9977) of serially diluted ULBP2 in 1% BSA–PBS detected using a conventional sandwich ELISA over a concentration range of 3.91 ng/mL–250 ng/mL.

shows the four-parameter dose-response relationship between the normalized fluorescence signal and the concentration of ULBP2 in 10-fold-diluted serum over the range from 0.1 pg/mL to 10 ng/mL. The correlation coefficient (R^2) was 0.9497, and the error bars represent one standard deviation for five repetitions. A LOD of 16 pg/mL in 10-fold-diluted human serum was obtained for the HT-LSPCHFB method.

In this study, the goal of the HT-LSPCHFB was to excite the harmonic intensity-modulated fluorescence signal, which can be measured precisely using a very narrow bandwidth filter via lock-in amplifier. Although a slight signal-to-noise ratio (SNR)

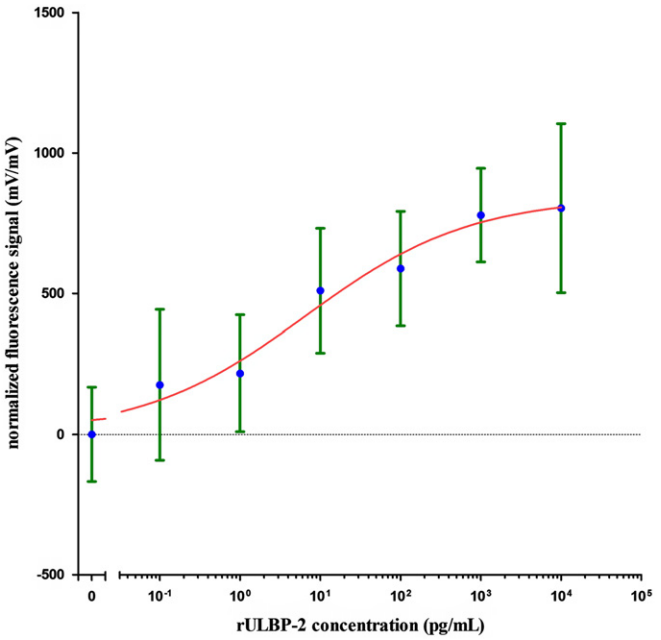

Fig. 4. The four-parameter dose–response relationship (R^2=0.9738) of serially diluted ULBP2 in 1% BSA–PBS detected by the HT-LSPCHFB over a concentration range of 0.1 pg/mL–10 ng/mL.

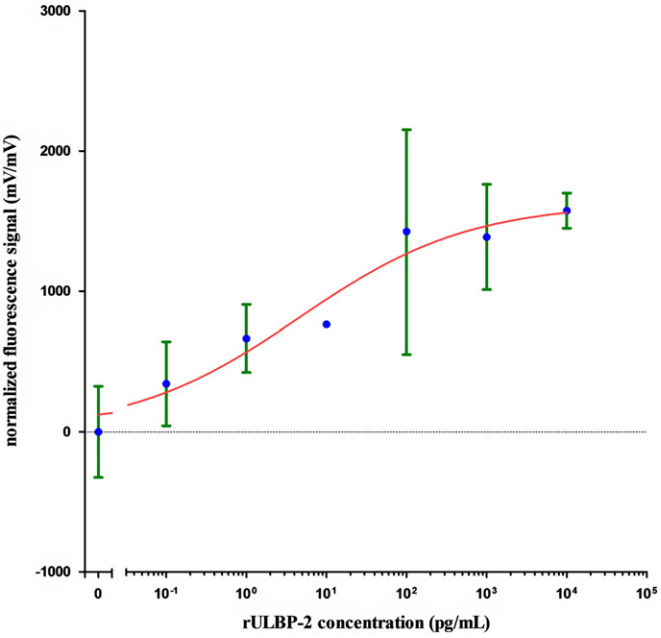

Fig. 5. The four-parameter dose-response relationship (R^2=0.9497) of serially diluted ULBP2 in 10-fold-diluted serum detected by the HT-LSPCHFB over a concentration range of 0.1 pg/mL–10 ng/mL.

improvement for the detected harmonic intensity-modulated fluorescence signal is resulted in contrast to the conventional fluorescence detection method, however, the simultaneous detection of the heterodyne fluorescence and reference signals by use of a two-frequency laser in association with the ratio algorithm significantly improves the SNR of the detected signal as shown in Fig. 2(A). This obviously enhances the sensitivity and stability of the biosensor. Because the binding of streptavidin to GNP is not covalent binding, a large uncertainty is expected during the measurement due to the large variation in the LSPCF probe during preparation via high speed centrifuge. The improvement of the immobilization of the detection antibody on GNP by changing to covalent binding is critical to the performance of the HT-LSPCHFB regarding the stability of the measurements.

Because PC is an insidious disease with no specific early clinical symptoms and with a high incidence of metastatic disease at the time of the initial diagnosis, its aggressive clinical course and the failure of systemic therapies are correlated (Chakraborty et al., 2011; Pliarchopoulou and Pectasides, 2009). In our previous study, using a cutoff value of 60 pg/mL for ULBP2, we demonstrated that the sensitivity and specificity for PC detection were 83.8% and 73.9%, respectively. Moreover, an analysis of the area under the receiver operating characteristic (ROC) curve showed that ULBP2 is superior to CA 19-9 in discriminating between PC patients with early-stage disease from healthy controls. Thus, a highly sensitive and high-throughput detection method is necessary to identify the small change in the ULBP2 concentration in human serum that will allow the early diagnosis of PC.

Currently, the detection of ULBP2 for PC diagnosis is limited because of its ultra-low levels in human serum (Chang et al., 2011b) and the LOD of conventional instruments, which generally hard to detect analytes in the pg/mL concentration range. To our knowledge, only a few groups have developed methods that are able to measure ULBP2 in human serum. They are the methods of (1) Steinle et al., who used a highly sensitive sandwich ELISA to detect soluble ULBP2 at 20 pg/mL using a high-performance and unusual antibody (Paschen et al., 2009; Waldhauer and Steinle 2006), and (2) Linkov et al. and Yu et al., who used integrated method involving a bead-based immunoassay and flow cytometry for which the LOD was at few pg/mL level for measuring ULBP2 level in human serum. However, ULBP2 was detectable fewer than 60% of the samples in Linkov et al.'s study (Chang et al., 2011b; Linkov et al., 2009). In our study, the HT-LSPCHFB was developed to create a method with high detection sensitivity for PC diagnosis utilizing human serum. The use of two identical polyclonal antibodies in the sandwich immunoassay used in the HT-LSPCHFB method not only increases the availability of antibody but also makes the method cost-effective for clinical diagnosis. Thus, the HT-LSPCHFB is comparable to the conventional bead-based immunoassay with respect to the cost-performance ratio. Because the HT-LSPCHFB method uses 96-well immunoplates, it can be used for parallel assays to improve the measurement efficiency. In the HT-LSPCHFB method, a scanning rate of $<$15 min/ 96 samples was used. Based on the high detection sensitivity and high-throughput capability of the HT-LSPCHFB for detecting ULBP2, this biosensor, in combination with CA 19-9 detection, could become a diagnostic tool for screening for pancreatic cancer.

4. Conclusions

In this study, a novel HT-LSPCHFB based on a two-frequency laser beam in conjunction with a 96-well immunoplate was proposed and analyzed. The HT-LSPCHFB uses two identical polyclonal antibodies in the sandwich immunoassay, in contrast to conventional methods in which two different types of antibodies are used. The use of one antibody not only increases the availability of antibody but also improves the efficiency of blood testing in clinical diagnosis. Experimentally, the HT-LSPCHFB can successfully detect human ULBP2 in 1% BSA–PBS or in 10-fold-diluted human serum, and the LOD of the HT-LSPCHFB is calculated to be 18 pg/mL in 1% BSA–PBS and 16 pg/mL in 10-fold-diluted human serum. Compared with the LOD of the conventional ELISA method, the LOD of the HT-LSPCHFB for ULBP2 detection is significantly improved by more than 100-fold when using the same antibody. Potentially, the HT-LSPCHFB could

become a high-sensitivity diagnostic tool for screening for PC, in combination with CA 19-9 detection, and for quantifying the serum levels of cancer markers in the near future.

Acknowledgments

This research was supported by the Ministry of Education, Aiming for the Top University Plan (EMRPD190041 and EMRPD1A0751). The National Science Council of Taiwan research grants (NSC 98–2221-E-182–063-MY3 and NSC 98-2221-F-182-064-MY3), the Chang Gung University research grant (UERPD2A0111) and the Chang Gung Memorial Hospital research grant (CMRPD290091) are also appreciated.

References

Anker, J.N., Hall, W.P., Lyandres, O., Shah, C., Zhao, J., Van Duyne, R.P., 2008. Nature Materials 7, 442–453.
Bausch, D., Thomas, S., Mino-Kenudson, M., Castillo, C.F., Bauer, T.W., Williams, M., Warshaw, A.L., Thayer, S.P., Kelly, K.A., 2011. Clinical Cancer Research 17, 302–309.
Bezabeh, T., Ijare, O.B., Albiin, N., Arnelo, U., Lindberg, B., Smith, I.C.P., 2009. Magnetic Resonance Materials in Physics, Biology and Medicine 22, 267–275.
Brand, R.E., Nolen, B.M., Zeh, H.J., Allen, P.J., Eloubeidi, M.A., Goldberg, M., Elton, E., Arnoletti, J.P., Christein, J.D., Vickers, S.M., Langmead, C.J., Landsittel, D.P., Whitcomb, D.C., Grizzle, W.E., Lokshin, A.E., 2011. Clinical Cancer Research 17, 805–816.
Chakraborty, S., Baine, M.J., Sasson, A.R., Batra, S.K., 2011. Biochimica et Biophysica Acta—Reviews on Cancer 1815, 44–64.
Chang, Y.-F., Chen, R.-C., Lee, Y.-J., Chao, S.-C., Su, L.-C., Li, Y.-C., Chou, C., 2009. Biosensors and Bioelectronics 24, 1610–1614.
Chang, Y.-F., Hung, S.-H., Lee, Y.-J., Chen, R.-C., Su, L.-C., Lai, C.-S., Chou, C., 2011a. Analytical Chemistry 83, 5324–5328.
Chang, Y.-F., Wang, S.-F., Huang, J.C., Su, L.-C., Yao, L., Li, Y.-C., Wu, S.-C., Chen, Y.-M.A., Hsieh, J.-P., Chou, C., 2010. Biosensors and Bioelectronics 26, 1068–1073.
Chang, Y.-T., Wu, C.-C., Shyr, Y.-M., Chen, T.-C., Hwang, T.-L., Yeh, T.-S., Chang, K.-P., Liu, H.-P., Liu, Y.-L., Tsai, M.-H., Chang, Y.-S., Yu, J.-S., 2011b. PLoS One 6, e20029.
Goggins, M., 2011. Clinical Cancer Research 17, 635–637.
Hartland, G.V., 2011. Chemical Reviews 111, 3858–3887.
Ho, J.-A.A., Chang, H.-C., Shih, N.-Y., Wu, L.-C., Chang, Y.-F., Chen, C.-C., Chou, C., 2010. Analytical Chemistry 82, 5944–5950.
Hsieh, B.-Y., Chang, Y.-F., Ng, M.-Y., Liu, W.-C., Lin, C.-H., Wu, H.-T., Chou, C., 2007. Analytical Chemistry 79, 3487–3493.
Huang, J.C., Chang, Y.-F., Chen, K.-H., Su, L.-C., Lee, C.-W., Chen, C.-C., Chen, Y.-M.A., Chou, C., 2009. Biosensors and Bioelectronics 25, 320–325.
Jones, M.R., Osberg, K.D., Macfarlane, R.J., Langille, M.R., Mirkin, C.A., 2011. Chemical Reviews 111, 3713–3735.
Li, C., Simeone, D.M., Brenner, D.E., Anderson, M.A., Shedden, K.A., Ruffin, M.T., Lubman, D.M., 2009. Journal of Proteome Research 8, 483–492.
Linkov, F., Gu, Y., Arslan, A.A., Liu, M., Shore, R.E., Velikokhatnaya, L., Koenig, K.L., Toniolo, P., Marrangoni, A., Yurkovetsky, Z., Zeleniuch-Jacquotte, A., Lokshin, A.E., 2009. European Cytokine Network 20, 21–26.
Ng, M.-Y., Liu, W.-C., 2009. Optics Express 17, 5867–5878.
Paschen, A., Sucker, A., Hill, B., Moll, I., Zapatka, M., Nguyen, X.D., Sim, G.C., Gutmann, I., Hassel, J., Becker, J.C., Steinle, A., Schadendorf, D., Ugurel, S., 2009. Clinical Cancer Research 15, 5208–5215.
Pliarchopoulou, K., Pectasides, D., 2009. Cancer Treatment Reviews 35, 431–436.
Rycenga, M., Cobley, C.M., Zeng, J., Li, W., Moran, C.H., Zhang, Q., Qin, D., Xia, Y., 2011. Chemical Reviews 111, 3669–3712.
Sagle, L.B., Ruvuna, L.K., Ruemmele, J.A., Van Duyne, R.P., 2011. Nanomedicine 6, 1447–1462.
Soo, P.-C., Horng, Y.-T., Chang, K.-C., Wang, J.-Y., Hsueh, P.-R., Chuang, C.-Y., Lu, C.-C., Lai, H.-C., 2009. Molecular and Cellular Probes 23, 240–246.
Su, D.-C., Chiu, M.-H., Chen, C.-D., 1996. Precision Engineering 18, 161–163.
Su, L.-C., Chang, Y.-F., Chou, C., Ho, J.-A.A., Li, Y.-C., Chou, L.-D., Lee, C.-C., 2011. Analytical Chemistry 83, 3290–3296.
Waldhauer, I., Steinle, A., 2006. Cancer Research 6, 2520–2526.
Willets, K.A., Van Duyne, R.P., 2007. Annual Review of Physical Chemistry 58, 267–297.
Yu, C.-J., Lin, C.-E., Teng, H.-K., Tsai, C.-C., Chou, C., 2008. Optics Communications 282, 1516–1520.
Yu, C.-J., Lin, C.-E., Yu, L.-P., Chou, C., 2009. Applied Optics 48, 758–764.